Equilibrium configuration of magnetic trilayers

T. L. Fonseca and N. S. Almeida
Departamento de Física Teórica e Experimental, Universidade Federal do Rio Grande do Norte, 59072-970, Natal, RN, Brazil
(Received 27 June 1997)

We use a simple and realistic theoretical model to investigate the equilibrium configuration of ferromagnetic-nonmagnetic-ferromagnetic trilayer systems. We assume the ferromagnetic films have a crystalline anisotropy and interact via bilinear and biquadratic coupling. We consider the system is always in the configuration that gives the absolute minimum to the energy to construct field-dependent phase diagrams for the case that the external dc field (H_0) is applied parallel to the surface of the films. We show that for a given value of the dc field, the equilibrium configuration has a peculiar dependence on the parameters that describe the anisotropy (H_a), bilinear (H_x), and biquadratic (H_b) coupling. We present general results for different values of H_b/H_x and H_a/H_x and we specialize our numerical calculation to display theoretical results for physical properties of systems that have values of H_a, H_b, and H_x, suitable to fit the experimental parameters of Fe/Cr/Fe magnetic trilayers. We predict interesting behavior of the magnetization with the strength of the dc field when it is not applied parallel to an easy axis. [S0163-1829(98)00601-8]

Very often in the last decade, the experimental results of physical properties of systems consisting of two magnetic layers separated by a nonmagnetic spacer suggested physical behavior that challenged our basic knowledge of such simple systems. The oscillatory dependence of the coupling between magnetic films on the thickness of the nonmagnetic spacer,[1,2] the alignment of the magnetic moments at 90° with respect to each other observed in different metallic trilayers,[3,4] among others, have motivated several authors to look for explanation for these intriguing physical properties.[5–10] On the experimental side, the techniques frequently used for characterization of these systems are magneto-optical Kerr effect (MOKE), ferromagnetic resonance (FMR), and Brillouin light scattering (BLS). It should be remarked that, while MOKE gives information on the equilibrium configuration of the system, FMR and BLS supplement this information with details of the dynamical behavior of the system. In other words, MOKE gives information on the ''magnetic phase'' of the system and through the data obtained by FMR and/or BLS the dynamical behavior of the system can be analyzed.

The first step to understand the dynamical behavior of the system is to learn how the equilibrium configuration is affected by of the environment; in other words, how the equilibrium configuration is modified by changes of the temperature, applied field, etc. It is known that, if the temperature of a magnetic multilayer system is modified, the magnetic coupling changes and the experimental data obtained by BLS or FMR must give information on the modifications of the intrinsic parameters.[11,12] It is also well known that, even if the temperature remains constant, an external dc magnetic field can modify the behavior of the system, and may give it entirely different physical properties. For a convenient choice of the parameters (thickness of the films and spacer), a small variation of the direction and/or strength of an externally applied field may modify significantly the response of the system to an external input. This might be of the interest in the development of devices like magnetic sensors.

Recently Azevedo *et al.*[13] presented a series of experimental results obtained by MOKE, FMR, and BLS for a Fe(40 Å)/Cr(15 Å)/Fe(40 Å) sample, grown by magnetron sputter deposition in a UHV chamber onto MgO(001). From their results one can appreciate the rich variety of magnetic phases of this system. They use a simple model to interpret their experimental data and, with the same set of parameters, they successful fitted the data obtained in all experiments mentioned above. In their model they assume that, besides the crystalline anisotropy and interfilm exchange interaction of the Heisenberg form $[H_x(\mathbf{n}_1\cdot\mathbf{n}_2)]$, the films also interact through a biquadratic coupling $H_b(n_1\cdot n_2)^2$, $H_b\geqslant 0$. The biquadratic coupling was observed some years ago by Rühring *et al.*[3] and, shortly after, Slonczewski[10] proposed intrinsic and extrinsic mechanisms that lead to this kind of coupling. When the biquadratic coupling was first observed, it was found to be rather weak, compared to the bilinear exchange H_x. However, it has been found that the Fe/Cr(211) structures might have the ratio $h_b=H_b/H_x$ quite large. This fact suggests that one may synthesize samples for which h_b can be adjusted to have the value appropriate for any particular purpose.

We should mention that the system studied here is equivalent to an infinite magnetic superlattice with similar parameters. The aim of this work is to present a theoretical study of the influence of the combined effects of the biquadratic coupling and crystalline anisotropy on the phase diagram of trilayer system. We will also show that the magnetic phases of these systems can be completely characterized by measurement of the magnetization and/or resonances of the system. This paper can be seen as an extension of Ref. 14, where the influence of the biquadratic exchange on the phase diagram of magnetic finite and infinite superlattice was studied. In that paper the authors considered that the magnetic multilayer systems had an uniaxial anisotropy and they predicted striking field-dependent magnetic phase diagrams. However, some of these systems have a very weak uniaxial anisotropy[15] or it does not appear at all.[13] On the other hand, it has been observed that in Fe/Cr/Fe structures grown onto

GaAs(100) or onto MgO(100), a crystalline anisotropy is always present. Therefore, to have a better comprehension of these system, the contribution of the crystalline anisotropy for the internal energy must be included in the energy functional of Ref. 14. In order to investigate the effects of this anisotropy on the magnetic phase diagram, we replace the term of the uniaxial anisotropy in Eq. (2.1) of Ref. 14, by

$$\frac{H_a}{2}\sum_{i=1,2}\{(n_i^x n_i^y)^2+(n_i^x n_i^z)^2+(n_i^y n_i^z)^2\}.$$

The presence of this anisotropy gives to the system a totally different symmetry (and consequently a quite different behavior) and it is responsible for the main characteristics of the physical properties reported in this paper.

The system under investigation is constituted by two infinitely extended thin ferromagnetic films (a few atomic monolayers), with static magnetization in-plane, separated by a nonmagnetic spacer. We define $\hat{n}_i$ as a unit vector in the direction of the magnetization of the ith film ($i=1,2$), and then we write the energy functional as

$$\begin{aligned}E(\hat{n}_1,\hat{n}_2)=&H_x\hat{n}_1\cdot\hat{n}_2+H_b(\hat{n}_1\cdot\hat{n}_2)^2-H_0\hat{n}_H\cdot(\hat{n}_1+\hat{n}_2)\\&+\frac{H_a}{2}\sum_{i=1,2}[(n_i^x)^2(n_i^y)^2+(n_i^x)^2(n_i^z)^2\\&+(n_i^y)^2(n_i^z)^2]+2\Pi m_s[(\hat{n}_1^{\perp})^2+(\hat{n}_2^{\perp})^2].\end{aligned}\quad(1)$$

In Eq. (1) the energy is given in units of magnetic field and the first term is the regular bilinear exchange which gives to the system a antiferromagnetic (ferromagnetic) character if H_x is positive (negative). The second term is the biquadratic exchange that has been found always positive ($H_b>0$). The third term is the Zeeman energy where we are assuming that the external dc magnetic field is applied parallel to $\hat{n}_H$. The fourth term is the crystalline anisotropy that defines the x, y, and z directions as the easy axis of the system. Finally, the last term is the surface anisotropy. In this term m_s denotes the saturation magnetization of the layer and $(m_s\hat{n}_i^{\perp})$ is the component of the magnetization perpendicular to the surface of the layer i. The approach used here can be used for any particular values of H_x, H_b, and H_a but in our numerical calculations we will always consider all of them positive.

We assume the demagnetization field generated by tipping the magnetization out of plane is strong enough to suppress any tendency of the equilibrium magnetization to tilt out of plane. Therefore, *in the equilibrium*, the magnetization of both films lie in the plane parallel to the surface and we define the direction perpendicular to the film as the y direction to write the unit vectors $\hat{n}_1=\hat{x}\cos(\theta_1)+z\sin(\theta_1)$, $\hat{n}_2=\hat{x}\cos(\theta_2)-\hat{z}\sin(\theta_2)$, $[\hat{n}_i^{\perp}=0\ (i=1,2)]$, and $\hat{n}_H=\hat{x}\cos(\theta_H)+\hat{z}\sin(\theta_H)$. Here the x and z directions are parallel to the surface of the films and the angles are measured from the x axis.

To obtain the equilibrium configuration, first we require that the energy functional be an extremum. Therefore, we must find solutions for the nonlinear set of equations

$$\begin{aligned}&\sin(\theta_1+\theta_2)+h_b\sin[2(\theta_1+\theta_2)]-\frac{h_a}{4}\sin(4\theta_1)\\&-h_0\sin(\theta_1-\theta_H)=0\end{aligned}\quad(2a)$$

and

$$\begin{aligned}&\sin(\theta_1+\theta_2)+h_b\sin[2(\theta_1+\theta_2)]-\frac{h_a}{4}\sin(4\theta_2)\\&-h_0\sin(\theta_2+\theta_H)=0.\end{aligned}\quad(2b)$$

In Eqs. (2), $h_b=H_b/H_x$, $h_a=H_a/H_x$, and $h_0=H_0/H_x$. The system of equations is solved by using the same approach used in Ref. 14 and here we will just mention the main steps. First we introduce the variables $\xi=\cos(\theta_1+\theta_2)$ and $\eta=h_a/2\sin(4\theta_1)+h_0\sin(\theta_1-\theta_H)$ to rewrite Eq. (2a) as

$$(1-\xi^2)(1+4h_b\xi+4h_b^2\xi^2)=\eta^2.\quad(3)$$

For a given θ_1 one can find values for $\theta_2(\theta_1)$ by solving Eq. (3) for ξ. Solutions for the problem are found when the values of θ_1 and θ_2, obtained from Eq. (3), are also the solution for Eq. (2b). The next step is to find out which solutions are the stable minimum. To do that we construct the matrix $M_{ij}=\partial^2E/\partial\theta_i\partial\theta_j$, ($i=1,2$) and we search, among the solutions, what are the angles that satisfy Eq. (2) and also give positive values for both eigenvalues of the matrix M. We notice that, for finite values of h_b, in general, there is more than one pair (θ_1,θ_2) that satisfy this requirement. To construct the field-dependent phase diagram we choose the solution that gives, for the fixed values of the parameters, the absolute minimum for $E(\hat{n}_1,\hat{n}_2)$. The borders of the phase are, in general, obtained numerically. However there are some special cases that analytical expressions can be found. For example, if H_0 is applied parallel to an easy axis, the antiferromagnetic phase is stable if $H_0^2\leqslant 2H_a(H_x-2H_b)+H_a^2$, while the ferromagnetic phase is stable for $H_0\geqslant 2H_x+4H_b-H_a$. The boundaries of the region where the spin-flop configuration is stable can be obtained from the calculation of the maximum and minimum values of H_0, that give real solutions for θ in the equation $2(h_a-4h_b)\cos^3(\theta)-(h_a-4h_b+2)\cos(\theta)+h_0=0$, and also give $8(h_a-4h_b)\cos^4(\theta)-4(1-2h_a+8h_b)\cos^2(\theta)+h_0\cos(\theta)+h_a-4h_b>0$.

In Figs. 1(a)–1(d) we show, for different values of $h_a=H_a/H_x$, the magnetic phase diagram for the case where the external dc field is applied parallel to the x axis (one of the easy axis). It should be said that the characteristic value of H_a for Fe films is 0.55 kG. The external dc field H_0, as well as the biquadratic exchange field H_b, are given in units of the bilinear exchange parameter H_x. In these figures is observed that, for small values of $h_b=H_b/H_x$ and $h_0=H_0/H_x$, the system has the magnetic moments aligned symmetrically with respect to the easy axis. This configuration characterizes the spin-flop phase. In this region of the h_0-h_b diagram, the spin-flop angles are between $\pi/4$ and $\pi/2$; i.e., the moments align between the hard axis and the easy axis perpendicular to the external field (z axis). In the diagrams we name this phase as SF1. For small but finite values of h_b, when h_0 is increased the system goes from the spin-flop configuration to the nonsymmetric phase (AS) with one of the magnetic moment aligned between the hard axis

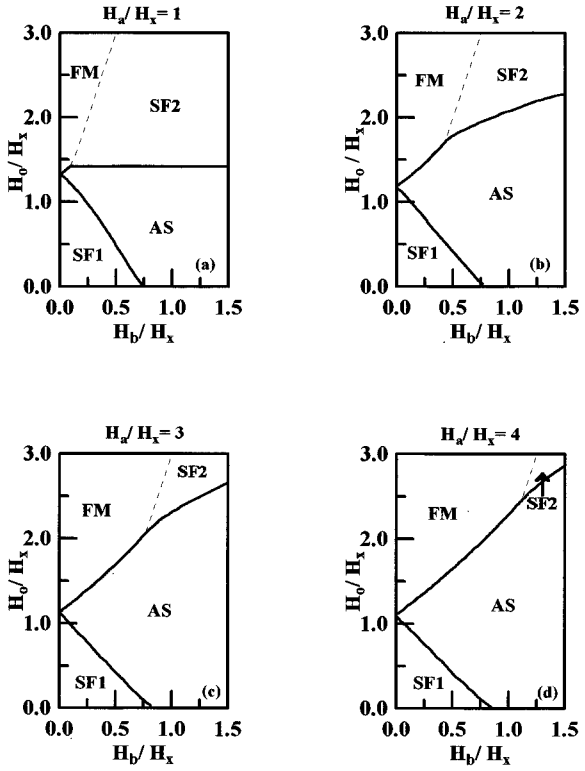

FIG. 1. h_0-h_b magnetic phase diagram of a trilayer system for H_0 parallel to the x axis and (a) $h_a=1$, (b) $h_a=2$, (c) $h_a=3$, and (d) $h_a=4$. The labels SF1, SF2, FM, and AS are defined in the text.

and the external field, while the other remains in a direction between the hard and z axis. The transition from SF1 to AS was always found to be of the first order. For $h_a>3$ and $h_b<0.75$, when h_0 is increased, both moments become aligned parallel to the external field after another first-order phase transition from the nonsymmetric (AS) to a ferromagnetic phase (FM). We emphasize that there are values of h_b for which the system goes to another spin-flop phase (SF2), after a first-order transition, before reaching the ferromagnetic phase. This spin-flop configuration (SF2) is similar to SF1 but in this case both moments point in directions between the dc field and the hard axis. For H_b smaller than H_x, this SF2 phase should be observed at a relatively low external dc field in samples for which $h_a<3$. The phase transition from SF2 to FM (when it does exist), is always of the second order. In the figures, dashed lines represent the frontier between phases that the phase transition is of the second order. It should be noted that, in all diagrams showed, there are tricritical points at particular values of h_b. We notice that these systems have interesting physical behavior around these points but it will not be discussed in this paper.

The phase diagrams have a quite different form when the external dc field is applied in an oblique direction with respect to an easy axis. We illustrate this fact by showing in Fig. 2(a) the phase diagram for the case where the angle between H_0 and the x axis is 20°. In Fig. 2(a) as well as in Fig. 2(b) we used $H_a/H_x=4$. In this geometry the system is also in the SF1 phase for small values of h_0 and h_b. When the external field is increased the system goes from SF1 to the AS phase after a first-order phase transition. The configu-

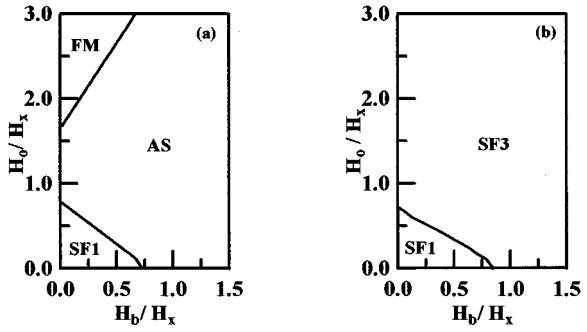

FIG. 2. h_0-h_b magnetic phase diagram of a trilayer system for $h_a=4$, and the angle between H_0 and the x axis equal to (a) 20°, (b) 45°. The labels are defined in the text.

ration in which both magnetic moments point in the same direction is reached after another first-order phase transition at higher value of h_0. It should be remarked that, in this phase, the angle between the magnetic moments and the external field is finite and decreases when the strength of the external field is increased. This angle goes to zero for a very high value of h_0. A singular behavior is observed in the phase diagram when the external field is applied parallel to the hard axis. We depict it in Fig. 2(b). In this arrangement, for small values of h_0 and h_b, the system is in the SF1 phase but this phase is degenerated; the configurations $\theta_1=\theta_2=\theta$ and $\theta_1=\pi/2+\theta$, $\theta_2=-\pi/2+\theta$ have the same energy. When h_0 is increased the system goes, after a first-order phase transition, to a configuration where the angles between the external field and the magnetic moments are equal $(\hat{n}_1\cdot\hat{n}_H=\hat{n}_2\cdot\hat{n}_H)$. We name this phase as SF3. The configuration that has the moments aligned parallel to the field is reached at high value of h_0 and the phase transition is of the second order.

There are several ways to observe the phase diagrams shown in Figs. 1 and 2. Probably the simplest experiments would be the direct measurement of the magnetization (through MOKE) and the measurement of the resonance frequency (FMR). The magnetization of the sample can easily be calculated from the equilibrium configuration. The resonance frequencies can be obtained from the equations of motion:

$$\frac{d\mathbf{m}_i}{dt}=\gamma\mathbf{m}_i\times\mathbf{H}^i_{\text{eff}} \tag{4}$$

with

$$\begin{aligned}\mathbf{H}^i_{\text{eff}}=&-[H_x+2H_b(\hat{n}_1\cdot\hat{n}_2)]\hat{n}_j-H_a\{n_i^x[(n_i^y)^2+(n_i^z)^2]\hat{x}\\&+n_i^y[(n_i^x)^2+(n_i^z)^2]\hat{y}+n_i^z[(n_i^x)^2+(n_i^y)^2]\hat{z}\}\\&+4\Pi m_s\hat{n}_i^{\perp}+\mathbf{H}_0,\end{aligned} \tag{5}$$

where $\hat{n}_i$ is the unit vector parallel to the magnetization of the film i and $\hat{n}_i^{\perp}$ is the unit vector perpendicular to the surface of the layer. A laborious but straightforward calculation gives the following expression for the resonance frequencies $(\mathbf{H}_0=H\hat{x})$:

$$\Omega_R^2=\frac{\gamma^2}{2}\{[A_1B_1+A_2B_2+2CD]\pm[(A_1B_1+A_2B_2+2CD)^2 - 4(A_1A_2-C^2)(B_1B_2-D^2)]^{1/2}\}, \quad (6)$$

where

$$A_i=H_x\cos(\theta_1+\theta_2)+2H_b\cos^2(\theta_1+\theta_2) - \frac{H_a}{2}[1+\cos^2(2\theta_i)]-H_0\cos(\theta_i)-4\Pi m_s, \quad (7a)$$

$$B_i=-H_x\cos(\theta_1+\theta_2)-2H_b\cos[2(\theta_1+\theta_2)] + H_a\cos(4\theta_i)]+H_0\cos(\theta_i), \quad (7b)$$

$$C=-H_x-2H_b\cos(\theta_1+\theta_2), \quad (7c)$$

and

$$D=H_x\cos(\theta_1+\theta_2)+2H_b\cos[2(\theta_1+\theta_2)]. \quad (7d)$$

We should notice that the frequencies given by Eq. (6) correspond to modes where the magnetic moments oscillate in phase (acoustical mode) and in opposite phase (optical mode). We choose $h_a=2$, $h_b=0.55$ to show, in Fig. 3, the behavior of the component of the magnetization parallel to H_0 (dashed line, right-hand y axis) and the absolute values of the difference between the frequencies of the acoustical and optical modes ($\Delta\Omega_R$) (full line, left-hand y axis) with the external field. From this picture one can see that, when the strength of the dc field approaches the values that make the system change the phase, the magnetization as well as $\Delta\Omega_R$ exhibit singular behavior. In particular, when the system exhibits a first-order phase transition, a discontinuity is observed in both quantities. Once again we should remark that the transition fields shown in the pictures were obtained by considering that the system is always in the configuration that gives the absolute minimum for the energy. In a laboratory the values of these fields should be slightly different if the transition is of the first order.

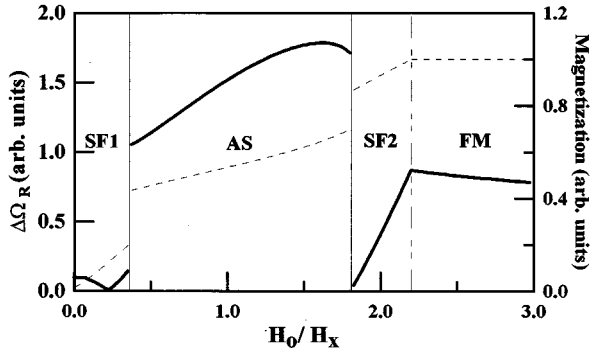

FIG. 3. For the case $h_a=2$, $h_b=0.55$, we show the variation of the difference $\Delta\Omega_R$ between the frequencies of the acoustical and optical modes with the external field h_0 applied parallel to the x axis (full line and y axis) and the behavior of the magnetization with h_0 under the same conditions.

We have shown that the magnetic-nonmagnetic-magnetic system with crystalline anisotropy and biquadratic exchange, in addition to the bilinear coupling, exhibits a rich variety of configurations induced by the external field. This kind of system has been grown, with very high quality, elsewhere and we hope the present calculation stimulate a detailed study of the remarkable capability of this system to display different physical properties.

The authors thank Dr. A. S. Carriço, Dr. A. Azevedo, and C. Chesman for helpful discussions. This research was partially supported by the Brazilian Agency CNPq.

[1] S. S. Parkin, N. More, and K. P. Roche, Phys. Rev. Lett. **64**, 304 (1990).
[2] See articles in, *Ultrathin Magnetic Structures I and II*, edited by J. A. C. Brand and B. Heirich (Springer, New York, 1994).
[3] M. Rührig, R. Schäfer, A. Hubert, J. A. Wolf, S. Demokritov, and P. Grünberg, Phys. Status Solidi A **125**, 635 (1991).
[4] C. J. Gutirrez, J. J. Krebs, M. E. Filipkowski, and G. A. Prinz, J. Magn. Magn. Mater. **116**, 1305 (1992).
[5] D. M. Edwards, J. Mathon, R. B. Muniz, and M. S. Phan, Phys. Rev. Lett. **67**, 493 (1991).
[6] D. M. Edwards, J. Mathon, R. B. Muniz, and M. S. Phan, J. Phys. Condens. Matter **3**, 4941 (1991).
[7] J. Mathon, M. Villeret, R. B. Muniz, J. d'Albuquerque e Castro, and D. M. Edwards, Phys. Rev. Lett. **74**, 3696 (1995).
[8] J. d'Albuquerque e Castro, J. Mathon, M. Villeret, and D. M. Edwards, Phys. Rev. B **51**, 12 876 (1995).
[9] S. Demokritov, E. Tsymbal, P. Grünberg, W. Zinn, and I. K. Schuller, Phys. Rev. B **49**, 720 (1994).
[10] J. C. Slonczewski, J. Magn. Magn. Mater. **150**, 13 (1995), and references therein.
[11] Z. Zhang, L. Zhou, P. E. Wigen, and K. Ounadjela, Phys. Rev. Lett. **73**, 336 (1994).
[12] N. S. Almeida, D. L. Mills, and M. Teitelman, Phys. Rev. Lett. **75**, 733 (1995).
[13] A. Azevedo, C. Chesman, S. M. Rezende, F. M. de Aguiar, X. Bian, and S. S. Parkin, Phys. Rev. Lett. **76**, 4837 (1996).
[14] N. S. Almeida and D. L. Mills, Phys. Rev. B **52**, 13 504 (1995).
[15] S. M. Rezende, M. A. Lucena, F. M. de Aguiar, A. Azevedo, C. Chesman, P. Kabos, and C. E. Patton, Phys. Rev. B **55**, 8071 (1997).